

Tension-Induced Mutual Adhesion and a Conjectured Superstructure of Lipid Membranes

W. HELFRICH

*Fachbereich Physik, Freie Universität Berlin,
Arnimallee 14, 14195 Berlin, Germany*

Contents

1. Introduction	693
2. Mutual adhesion of lipid membranes induced by lateral tension: experiments	695
3. Tentative theory of induced adhesion	705
4. The contradictions of induced adhesion	709
5. Other indications of lipid membrane complexity and superstructure	713
6. Conclusion	717
Acknowledgements	718
References	718

1. Introduction

Parallel fluid membranes in water repel or attract each other and the dependence of the forces on spacing can result in an equilibrium state of mutual adhesion. Attraction and adhesion are either spontaneous or induced by lateral tension. In induced adhesion, the tension acts by suppressing out-of-plane fluctuations, thus enabling Van der Waals attraction to prevail over repulsion by fluctuations and other repulsive interactions.

It is not clear whether the most common electrically neutral lipid membranes such as the bilayers of phosphatidylcholine (PC), phosphatidylethanolamine (PE) and digalactosylacylglycerol (DGDG) display spontaneous mutual adhesion. Some researchers inferred this from finding by X-ray diffraction a stationary maximum period of multilayer systems in excess water [1]. Studying giant vesicles, E. Evans and coworkers measured the mutual adhesion energies of PC, PE and DGDG membranes to be $(0.01 - 0.015)$ mJ/m², $(0.12 - 0.15)$ mJ/m² and 0.22 mJ/m², respectively [2, 3]. Our own experiments on lipid/water systems did not yield any evidence for mutual spontaneous adhesion of PC and PE bilayers. There appears to be a conflict between our results and those of Evans which needs to be resolved. It may be related to the fact that we did not mechanically disturb the membranes but only watched them under the microscope, while in Evans' studies giant vesicles were manipulated with micropipettes. However, we and Evans and many others utilized the spontaneous swelling of these lipids in water to obtain single membranes and vesicles.

A large amount of theoretical work has been devoted in recent years to the 'unbinding transition' of fluid membranes, i.e. the transition from mutual spontaneous adhesion to the unbound state, as some parameter is varied. These studies started with the renormalization group treatment by Lipowsky and Leibler [4] and were continued mostly by Lipowsky and his group [5], with a few contributions from others [6–9]. Lateral tension, which by definition is not required for spontaneous adhesion, was taken to be zero in these calculations. The renormalization group flow equations of fluid membranes with a bending stiffness in three dimensions are identical to those of stretched polymers in two dimensions [10]. Although the identity holds only to a first approximation [6, 8], it is often invoked since the polymer problem can be expressed exactly by a Schrödinger-type equation, thus allowing analytical solutions. Numerical studies and other theoretical methods all showed the equilibrium mean spacing $\langle z \rangle_{\text{eq}}$ of parallel undulating membranes to obey

$$\langle z \rangle_{\text{eq}} \sim (A_c - A)^{-\psi} \quad (1)$$

as the control parameter A approaches from below its critical value A_c where the membranes cease to adhere. The control parameter may be the strength of an attractive interaction potential ($A < 0$) or temperature ($A > 0$). The critical exponent

of unbinding is generally predicted to be $\psi = 1$ for a pair of adhering membranes. Recent numerical results suggest $\psi < 1$ for three and more equal membranes in mutual spontaneous adhesion [11], which is contested on analytical grounds in the case of stretched polymers [9].

On the experimental side, there is to date only one known example of an unbinding transition [12]. DGDG in 100 mM NaCl solution was found to swell indefinitely at elevated temperatures. Adjacent membranes went into spontaneous adhesion when subsequently the temperature was lowered. The reversible transition appeared to be continuous, but it was not possible to check the scaling law (1). The transition temperature varied wildly among seemingly equal samples and decreased slowly in the course of days. Spontaneous adhesion was never seen when no salt was present.

Adhesion induced by lateral tension occurs with PC, PE and DGDG bilayers [13–17]. Its accidental occurrence in highly swollen lipid samples is a rare phenomenon which we overlooked for years. Induced adhesion, unlike spontaneous adhesion, is characterized by contact angles of the adhering single membrane that are practically independent of lateral tension. In general, the tensions are below 10^{-3} mN/m so that they can be read from the contact rounding, i.e. a rounding of the membrane next to the area of adhesive contact. Contact angles are always less than 90° , as is necessary since the component of the tension parallel to the contact area has to be positive in the case of induced adhesion.

The experiments with DGDG in salt solution, showing both kinds of adhesion, confirmed that we had seen induced adhesion with PE and PC. Moreover, induced adhesion could be brought about willfully by two reversible procedures which were investigated with egg yolk PC (EYPC). One of them is osmotically controlled, the tension being generated by osmotic inflation of vesicles [14, 15]. The other is temperature controlled and operates in multilayer systems, the lateral tension resulting from membrane area contraction due to cooling. In both cases there was little or no dependence on salt concentration or initial temperature, which is direct evidence against spontaneous adhesion.

The theoretical treatment of mutual adhesion induced by lateral tension is difficult because of the simultaneous action of bending rigidity and lateral tension. We have tried to explain the experimental data in terms of undulatory repulsion, partially suppressed by tension, and attraction through a $1/z^2$ Van der Waals potential [14–16]. This approach leads to the scaling laws

$$\langle z \rangle_{\text{eq}}^2 \sim 1/\sigma \quad (2)$$

and

$$g_{\text{ad}} \sim \sigma, \quad (3)$$

where σ is the lateral tension and g_{ad} the adhesion energy between membranes per unit area of adhesive contact. A derivation of the same scaling laws, but for a different regime near the critical point of unbinding where the spacings are large, has been given by Lipowsky and Seifert [18]. Both (2) and (3) agree with the experimental

data, a coincidence regarded at first [14] as proof that the membranes are driven apart by the usual thermal undulations. However, a comparison of the values of the adhesion energy obtained from two different formulas, the Young equation and another energy balance, revealed discrepancies of two orders of magnitude. They forced us to postulate that at very low tensions (ca. 10^{-5} mN/m) the membranes store several times the excess area that is expected to reside in the undulations. This anomalous membrane roughness, in turn, requires for its support a membrane superstructure. In the meantime we have searched with more direct experimental methods for both superstructure and roughness.

The following is a review of our experiments on induced adhesion and their theoretical interpretation. There seems to be no similar work by other authors in the literature. At the end of the article we will compile additional evidence, direct or circumstantial, for a superstructure, an anomalous roughness or, generally, anomalous behavior of the lipid membranes investigated.

2. Mutual adhesion of lipid membranes induced by lateral tension: experiments

Accidental and osmotically controlled induced adhesion were studied in very dilute samples containing less than 1 wt% of lipid. To prepare a sample cell some μg of the material were put on an object slide and covered in general with twice distilled water. The samples had an area of a few cm^2 and a thickness of $100\ \mu\text{m}$ to $2\ \text{mm}$, depending on the experiment. After mounting the cover slip the cell was sealed with a glue or silicone grease to prevent evaporation. Giant vesicles and other extended membranes developed within hours or days. Their contours were studied by means of phase contrast light microscopy.

We first reported on accidental induced adhesion of EYPC bilayers at a meeting in Italy in 1982 [13]. The phenomenon was demonstrated by a picture of a fluctuating tubular vesicle adhering to a tight convex membrane. We inferred from it that stretching one of two membranes may be enough to induce adhesion between them. In this singular case of a free vesicle sticking to a stretched membrane, adhesion may have been promoted by the tubular geometry which restricts membrane undulations [19]. The lateral tension of the fluctuating membrane was estimated from contact rounding by use of the relationship

$$\xi_d^2 = \frac{\kappa}{\sigma} \quad (4)$$

which gives the deflection (or rounding) length ξ_d as a function of bending rigidity κ and lateral tension σ . Employing $\kappa = 2 \times 10^{-19}$ J, we computed $\sigma = 10^{-4}$ mN/m. A Young equation,

$$g_{\text{ad}} = (1 - \cos \psi)\sigma, \quad (5)$$

was used to obtain the adhesion energy g_{ad} per unit area from the contact angle ψ and the lateral tension of the fluctuating membrane.

Next, we tried to bring about induced adhesion by osmotic inflation of EYPC vesicles. For this purpose we exchanged the external aqueous medium to decrease the molarity of the NaCl or glucose solution (which at the beginning of the experiment was the same inside and outside the vesicles). Since the exchange swept away free vesicles, only those could be studied that were attached to the glass for unrecognizable reasons. Lowering the concentration by somewhere between 0.2 and 20% (larger changes led to membrane rupture), we were able to achieve induced adhesion between spherical vesicles. The areas of membrane adhesion originated from initial points of contact. An example is shown in fig. 1. Adhesion could sometimes be turned on and off several times by alternating the molarities. Also, it tended to disappear spontaneously within minutes or hours, but could be brought back by further reducing the molarity. The maximum contact angle of symmetric pair adhesion (see below) was 45° . Despite great efforts, no other information could be extracted from these poorly reproducible experiments. Failing to publish the results in *Nature*, we finally presented fig. 1 at a conference in the USA in 1985 and had it published in the proceedings [14].

We then engaged in an extensive study of accidental induced adhesion in very dilute PC samples, using mostly EYPC which was purchased from various sources. A comprehensive description of this work, including osmotically controlled adhesion, has been given in a journal article [15]. Examples of accidental induced adhesion are shown in figs 2–4. The most remarkable property of induced adhesion is the constancy of the contact angles. It could be verified over two orders of magnitude of the lateral tension for symmetric pair adhesion, i.e. two bilayers of equal ψ and σ forming a plane area of adhesive contact. The data are collected in fig. 5 where the adhesion energy is plotted versus the lateral tension. The latter was obtained from eq. (4) by inserting the rounding length and $\kappa = 2 \times 10^{-19}$ J. For the details of finding ξ_d we refer to the original paper. The adhesion energy was computed from the tension by use of the Young equation for symmetric pair adhesion

$$g_{\text{ad}} = 2(1 - \cos \psi)\sigma \quad (6)$$

which differs from (5) by the factor 2. Apart from some scatter, the points very nearly follow a slope of unity in the doubly logarithmic plot. This slope reflects the constancy of the contact angle which on average was 40° (ψ never exceeded 45° and rarely was below 30°). A constant angle ψ in (6) entails the scaling law (3).

Besides symmetric pair adhesion we concentrated on the adhesion of a single membrane to a bundle of n other membranes in the limit of large n . The contact angle of the single membrane increases with n to reach its maximum of 70° practically at $n = 6$, while the contact angle of the bundle goes to zero at the same time. Evidently, for $n \geq 6$, the system is like a single membrane adhering to a rigid wall so that the relevant Young equation is (5) instead of (6).

Fig. 1. Osmotically controlled induced adhesion of EYPC vesicles attached to glass slide. The same vesicles (a) in 156 mOsm NaCl solution prior to osmotic inflation, (b) in 131 mOsm after first inflation, and (c) in 131 mOsm after third inflation and spontaneous ceasing of adhesion. (Before the last picture, adhesion was turned on and off 3 and 2 times, respectively, by alternating between 156 and 131 mOsm.)
The bar represents 10 μm .

Fig. 2. Accidental induced adhesion of dimyristoyl phosphatidylcholin (DMPC) membranes. Evolution with time of an adhesive contact of two membranes. The left membrane displays contact rounding in (a), (c) and (d). Symmetric adhesion without visible contact rounding is seen in (b). The bar represents $10 \mu\text{m}$.

Fig. 3. A 'branched' structure of EYPC membranes displaying induced adhesion. There is symmetric pair adhesion and the adhesion of single membranes to bundles. Contact roundings are well visible. The bar represents 10 μm .

Fig. 4. Induced adhesion of dimyristoyl phosphatidylethanolamine (DMPE) membranes. One sees the same phenomena as in fig. 3. Some of the contact angles are on the low side for PE. The bar represents 10 μm .

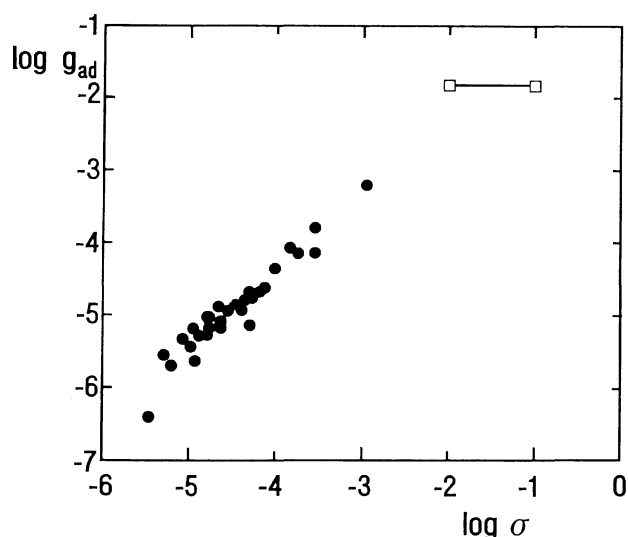


Fig. 5. Adhesion energy g_{ad} of symmetric pair adhesion induced by lateral tension plotted vs. lateral tension σ . The units are mJ/m^2 and mN/m , respectively. The point at $\sigma = 10^{-3}$ mN/m represents DMPC, all others EYPC. See text for explanations. The open boxes indicate the results of Evans and Metcalfe for EYPC which were measured with the tension of the more flaccid membrane being between 10^{-2} and 10^{-1} mN/m .

EYPC in 30 to 100 mM NaCl solution swelled more slowly and the swollen structures were smaller than in pure water. The contact angles of induced adhesion were still measurable and found to be the same as with pure water. This indicates that the induced adhesion in our samples was not affected by electrostatic repulsion, so that the absence of spontaneous adhesion is most likely not a consequence of electric surface charges. A few experiments with dimyristoyl PC (DMPC) in pure water showed the contact angle of symmetric adhesion to be the same as with EYPC. However, accidental induced adhesion was much rarer than in the case of EYPC.

Later on, accidental induced adhesion was investigated for PE and DGDG bilayers [17]. The results do not differ from those obtained with PC, except for slightly larger contact angles. The two PEs studied, dimyristoyl and dilauroyl (DMPE and DLPE), swelled easily up to at least 100 mM NaCl and had equal contact angles which did not change with salt concentration. The contact angles of induced adhesion were registered for both symmetric pair adhesion and adhesion of a single membrane to

Table 1
Average contact angles of induced adhesion (in degrees).

	PC	PE	DGDG
symmetric pair	40	45	55
single membrane to stack	70	80	85

Fig. 6. Induced adhesion brought about by cooling. The picture shows EYPC myelin cylinders in a sample being cooled after swelling at 55 °C. The three curved cylinders span the 20 μm thick sample cell; the white center lines are their water cores. Actually, one sees three sections of the same folded cylinder which is attached to a planar multilayer system. The PC density in the planar system is ca. 45 vol.%. The bar represents 20 μm . The instantaneous temperature is 51°C. Note the oblique white lines, the first sign of induced adhesion.

a stack of adhering membranes. The average contact angles of PC, PE and DGDG bilayers are compiled in table 1.

In all the studies of accidental induced adhesion we changed between at least two different glues or a glue and a silicon grease without noticing an effect on the contact angles.

Induced adhesion of EYPC bilayers may have been seen also by Israelachvili, Zasadzinski and coworkers [20]. They studied small vesicles of diameters near 100 nm, osmotically inflated or not, in freeze fracture electron microscopy and found adhesive contacts between them. The contact angles of symmetric pair adhesion were similar to those of our experiments. The results were explained in terms of an attractive hydrophobic interaction between stretched membranes which is proportional to lateral tension [21]. The proportionality agrees with (3), but the interaction is ‘direct’, i.e. relating to flat membranes without any undulations. Ignoring undulations and other

Fig. 7. Same as in fig. 6, but the instantaneous temperature is 45 °C. Note the compartments (white) separated by membrane bundles (dark).

roughness seems dangerous as it would imply a collapse of unstressed membranes into a bound state of (slightly) increased membrane area.

In addition to the osmotic inflation of vesicles there is another kind of controlled induced adhesion which was observed in swollen multilayer systems. It is brought about by cooling and was studied only with EYPC in pure water [16]. To achieve fairly uniform alignment of the membranes parallel to the glass, the samples were prepared by squeezing the slightly hydrated lipid between the slides to a thickness of about 20 μm . The remaining 90% of the cell volume were filled with twice distilled water. Mechanical sealing obviated the use of a glue. The local lipid density and thus the mean membrane spacing could be monitored during the swelling process by measuring the intensity of EYPC fluorescence.

The adhesion caused by cooling has been described in the second of a series of light-microscopic studies of swollen EYPC multilayer systems. The first deals with the swelling process and, in particular, with the generation of myelin cylinders spanning the sample cells up to a thickness of 40 μm [22]. The third reports on the 'dark bodies' which appear in about half of the swollen multilayer systems as soon as they are cooled [23]. In the second we describe the other half that display only

Fig. 8. Induced adhesion brought about by cooling. The picture shows the semicylindrical border of an EYPC planar multilayer system. There is a stray membrane on the side of free water. The $18\ \mu\text{m}$ thick sample is being cooled after swelling at 65°C . The PC density in the planar system is ca. 40 vol.%. The bar represents $20\ \mu\text{m}$. The instantaneous temperature is ca. 55°C . Note the white islands in the border, the first sign of induced adhesion.

induced adhesion. An example of induced adhesion caused by cooling is shown

Fig. 9. Same as in fig. 8, but the instantaneous temperature is 25°C . Note the increased width of the border and the numerous branchings. Some of the thinnest dark lines are single membranes.

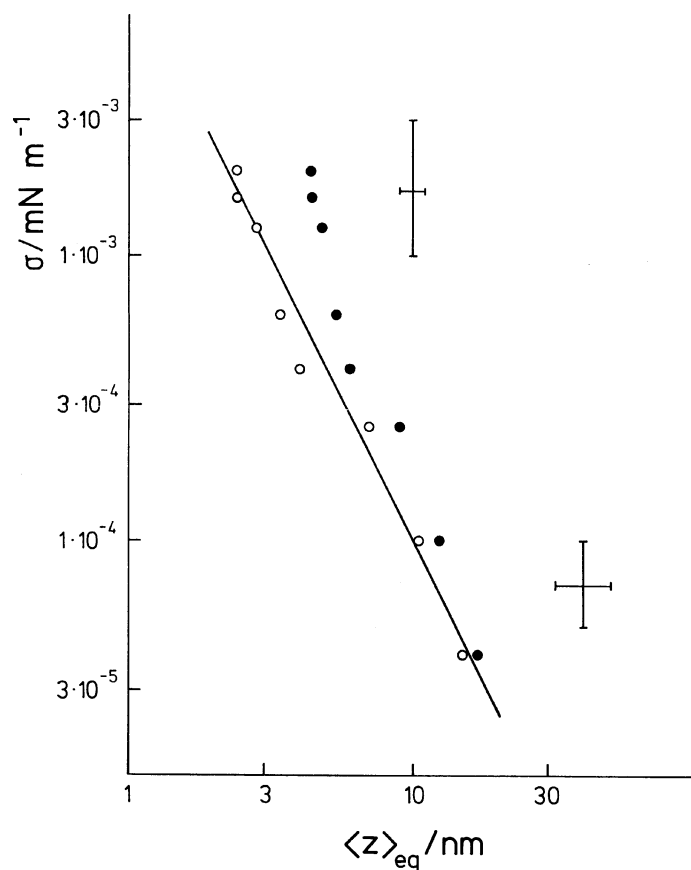


Fig. 10. Doubly logarithmic plot of lateral tension σ vs. equilibrium mean membrane spacing $\langle z \rangle_{\text{eq}}$ in the planar multilayer system. The solid dots are the raw data, the open dots result from an arbitrary increase of the membrane thickness from 3.8 to 5.8 nm. The straight line represents the scaling law (2).

in figs 6 and 7 which depict a myelin cylinder photographed at two subsequent moments as the temperature was dropping. The most interesting sample regions were the semicylindrical borders of the planar multilayer systems (which form myelin cylinders when folded). They were wider than half the sample thickness, the width increasing with decreasing temperature, as is illustrated by figs 8 and 9. The widened semicylinders permitted us to discern single membranes, read their contact angles and rounding lengths, and measure the thickness of stacks, i.e. thick bundles of many mutually adhering membranes. The average contact angle of a single membrane adhering to a stack was found to be 70° , thus equaling the contact angle of accidental adhesion to a bundle of six or more membranes. Temperature controlled induced adhesion is reversible, leaving no visible traces when the temperature differences are small enough.

The lateral tension inducing adhesion in swollen multilayer systems results from the membrane area contraction which accompanies cooling. Decreasing the temperature by a few K was usually sufficient to produce first signs of adhesion in the semicylindrical border. Even when several times larger, the decreases did not result in tensions strong enough to induce adhesion in the planar regions of the multilayer system. This can be explained by a complicated theoretical model predicting the tension to be self-limiting [16]. An important parameter of the model is the thermal area expansivity of the bilayer which was measured by Evans to be $2.4 \times 10^{-3} \text{ K}^{-1}$ for EYPC [24]. In its asymptotic limit the tension is just strong enough to neutralize membrane interaction in the planar multilayer system, thus facilitating the necessary restructuring. A check of the model consists in adding up the widths of the separate stacks in the semicylindrical border. When this could be done the total width equaled half the sample thickness, in agreement with the model. Identifying $\langle z \rangle_{\text{eq}}$ with the mean membrane spacing in the planar multilayer system and estimating σ from the contact rounding, we were able to obtain the lateral tension as a function of the equilibrium spacing produced by it.

Data obtained from different samples are collected in fig. 10. The tensions were calculated from (4), this time with $\kappa = 1 \times 10^{-19} \text{ J}$. The scaling law (2) was reproduced when an impenetrable layer of 2 nm was added to the assumed membrane thickness of 3.6 nm, which is a primitive way of dealing with hydration forces (see below). Although the proof of the scaling law may be doubted because of the large experimental errors, the orders of magnitude, $\langle z_{\text{eq}} \rangle = 10 \text{ nm}$ at $\sigma = 10^{-4} \text{ mN/m}$, seem reliable, apart from the uncertainty of κ that is reflected in an equal uncertainty of σ .

3. Tentative theory of induced adhesion

There is little theoretical work on adhesion induced by lateral tension. In all of it, standard thermal undulations are the only membrane roughness taken into account. We tried to explain induced adhesion in terms of the interplay of Van der Waals attraction and undulatory repulsion. The Van der Waals interaction energy per unit area between two flat membranes in the half-space approximation is

$$g_{\text{vdw}} = - \frac{H}{12\pi z^2} \quad (7)$$

where H is the Hamaker constant. This approximation is thought to be good up to rather large spacings, the true value falling below 50% of (7) only at $z \approx 20 \text{ nm}$ [25]. The wide range of applicability of (7), due to the enormous difference in dielectric constant between water and hydrocarbon, presupposes an unscreened zero frequency contribution. The finite membrane thickness makes Van der Waals attraction drop with $1/z^4$ at larger spacings. Repulsive short-range forces, called hydration forces, dominate at spacings below ca. 3 nm [26]. The undulations produce a repulsive interaction which was calculated by various methods for multilayer systems in the ideal case of purely steric interaction. In the earliest calculation, which integrates

over fluctuation modes and uses a self-consistency relation, the energy of undulatory interaction per unit area was found to be

$$g_{\text{und}} = \frac{3\pi^2}{128} \frac{(kT)^2}{\kappa \langle z \rangle^2}, \quad (8)$$

$\langle z \rangle$ being the mean spacing imposed by an external constraint [27]. The formula, in particular the numerical factor, was experimentally confirmed within 20% for very flexible nonlipid bilayers [28, 29]. However, the theoretical strength of undulatory interaction came out smaller in other treatments [30]. It is about 2/3 as large if a sum over the membranes is taken instead of an integral in z direction [31] and about 1/2 as large as (8) in Monte Carlo simulation [32] and renormalization group calculations [33]. Note that both interaction energies, (7) and (8), vary as the inverse square of spacing, z being fixed in one case and averaged in the other.

A formula like (8), but with a poor numerical factor, can be obtained from an ‘independent membrane piece’ approximation [13, 16]. For simplicity, one considers here a single membrane between parallel rigid walls of distance $2d$. The idea of the approximation is to cut the membrane into equal pieces, e.g., squares, so that the thermal undulations of each piece fill a certain fraction of the interval between the walls. Assuming the pieces to act as the particles of a one-dimensional ideal gas, one arrives at the pressure exerted on the wall by the undulating membrane.

It is an advantage of the independent membrane piece approximation that lateral tension can be taken into account in calculating the mean square fluctuation amplitude $\langle u^2 \rangle$ of the quadratic piece [13, 16]. Assuming a square of area S with periodic boundary conditions, one has for a single undulation mode of wave vector \vec{q} the mean square amplitude

$$\langle |u_{\vec{q}}|^2 \rangle = \frac{kT}{(\sigma q^2 + \kappa q^4)S}. \quad (9)$$

Integration over the \vec{q} plane leads to

$$\langle u^2 \rangle = \frac{kT}{4\pi\sigma} \ln \left(1 + \frac{\sigma}{\kappa q_{\text{min}}^2} \right) \quad (10)$$

where the lower wave vector cutoff is, to a good approximation, given by

$$q_{\text{min}}^2 = \frac{\pi^2}{S}, \quad (11)$$

and the upper wave vector cutoff need in general not be considered. Taking the limit of (10) for $\sigma \rightarrow 0$ gives the correct result for $\sigma = 0$. The area S as a function of σ may be obtained by assuming

$$\langle u^2 \rangle = \frac{d^2}{6}, \quad (12)$$

where $d^2/6$ is the geometric mean of the mean square fluctuation amplitudes of a simple sine wave ($\sin qx$) and a product wave ($\sin qx \sin qy$), both restricted to the interval $2d$ [13–15]. Eliminating $\langle u^2 \rangle$ between (10) and (12), one finds

$$S(\sigma) = \frac{\pi^2 \kappa}{\sigma} \left[\exp \left(\frac{2\pi\sigma d^2}{3kT} \right) - 1 \right] \quad (13)$$

which has to be inserted in

$$P_{\text{und}} = \frac{kT}{S(\sigma)2d} \quad (14)$$

to obtain the undulation pressure P_{und} on the walls. The effect of σ on S and, thus, P_{und} becomes significant when the exponent in (13) approaches unity. In the limit $\sigma \rightarrow 0$ a first order expansion of the exponential function leads to $S(0) \sim \langle z \rangle^2$ as expected. The ratio $S(0)/S(\sigma)$ may be regarded as the reduction factor of the undulation pressure in the presence of tension.

Since we are interested in a multilayer system rather than a membrane between rigid walls we apply this reduction factor to the undulation pressure derived from (8), writing

$$P_{\text{und}}(\sigma) = - \frac{\partial g_{\text{und}}}{\partial \langle z \rangle} \frac{S(0)}{S(\sigma)}. \quad (15)$$

Let us now superimpose P_{und} and the Van der Waals pressure P_{vdw} derived from (6),

$$P_{\text{vdw}} = - \frac{\partial g_{\text{vdw}}}{\partial z} = - \frac{H}{6\pi z^3} \quad (16)$$

and calculate the equilibrium spacing $\langle z \rangle_{\text{eq}}$ from

$$P_{\text{vdw}} + P_{\text{und}} = 0. \quad (17)$$

If one puts $z = \langle z \rangle_{\text{eq}}$, the result is

$$\frac{S(\sigma)}{S(0)} = \frac{9\pi^3(kT)^2}{32H\kappa}. \quad (18)$$

Replacing d by $\langle z \rangle_{\text{eq}}$ and expanding the exponential up to second order, one obtains from (13)

$$\frac{S(0)}{S(\sigma)} = 1 - \frac{\pi\sigma}{3kT} \langle z \rangle_{\text{eq}}^2 \quad (19)$$

is first order in $\sigma\langle z \rangle^2$. Combination of the last two equations results in

$$\langle z \rangle_{\text{eq}}^2 = \frac{H_c - H}{H} \frac{3kT}{\pi\sigma} \quad (20)$$

if use is made of the ‘critical’ Hamaker constant $H_c = (9\pi^3/32)(kT)^2/\kappa$ for which (17) holds with $\sigma = 0$. The ensuing scaling law

$$\langle z \rangle_{\text{eq}}^2 \sim 1/\sigma \quad (21)$$

is not only a consequence of the expansion but follows generally from $S(0)/S(\sigma)$ as given by (13). It also seems to follow from Sornette’s renormalization group treatment of undulatory membrane repulsion in the presence of lateral tension [34]. Insertion of (21) into the half-space potential (7) results in the scaling law relating adhesion energy to lateral tension,

$$g_{\text{ad}} \sim \sigma. \quad (22)$$

We refrain from writing down an explicit formula for g_{ad} . Any differences between pairs, bundles and multilayer systems of membranes should not affect the scaling laws. Note that (21) and (22) are identical to (2) and (3), respectively.

A completely independent argument confirms the scaling laws (21) and (22) [15]. It is based on the observation that the undulations of a single membrane bound by an attractive $1/z^2$ potential are characterized by two lengths. These are the deflection length defined by (1) and the lateral correlation length ξ which apart from a numerical factor near unity satisfies

$$\xi^2 = \frac{\kappa}{kT} \langle z \rangle_{\text{eq}}^2. \quad (23)$$

The ratio of the two lengths should depend only on the ratio H/H_c , so that

$$\xi^2/\xi_{\text{d}}^2 = \frac{\sigma}{kT} \langle z \rangle_{\text{eq}}^2 = f(H/H_c), \quad (24)$$

which immediately entails (21) and (22). A detailed way of proving the two identities of (24) is to consider a deformed membrane pieces, multiply their lengths either including or excluding z by the same factor, and require the energies of bending, pulling in area, and of the Van der Waals interaction (7) to be invariant. Note that the bending rigidity enters neither the exponent in (13) nor the length ratio in (24).

The confirmation of the scaling laws (21) and (22) by the direct argument of the last paragraph is welcome since the superposition of potential and undulatory energies is not necessarily correct, neither quantitatively nor qualitatively [4]. In the explicit equations, however, the errors of the numerical factors and the critical Hamaker constant are probably large. Uncertainties concerning the validity of the bare scaling laws arise from the use of the half-space law (7) which is only an approximation of the real Van der Waals interaction.

It has been shown above that the experimental data about induced adhesion agree very well with the scaling law (21) or (2) and are compatible with the scaling law (22) or (3). The twofold conformity seems to prove that induced adhesion can be fully understood in terms of standard thermal undulations besides Van der Waals attraction. However, this early conclusion [14] had to be dropped later on in view of conflicting numbers obtained from two different formulas for the adhesion energy [15]. Also, the measured equilibrium spacings seem too small, at the estimated tensions, to be compatible with undulation theory [16]. These discrepancies are to be examined next.

4. The contradictions of induced adhesion

In discussing the contradictory formulas for the adhesion energy we at first assume, as is common in the theory of elasticity, that the changes in membrane area can be neglected in calculating elastic energy densities. To this approximation, the adhesion energy per unit area of a single membrane adhering to a stack of membranes satisfies the energy balance

$$g_{\text{ad}} = g_{\text{f}} - g_{\text{b}} \quad (25)$$

besides the Young equation (5). Here g_{f} and g_{b} are the energies of the free and bound states, respectively, per unit area of membrane. For symmetric pair adhesion, the right sides of (5) and (25) have to be multiplied by 2 and g_{ad} and g_{b} may change somewhat (which we do not express by different symbols). With induced adhesion all three energy densities depend on lateral tension. If one wants to be precise, one has to distinguish between the tensions σ_{b} and σ of the membrane where it is bound and free, respectively. They are related by

$$\sigma_{\text{b}} = \sigma \cos \psi. \quad (26)$$

We do not make here this distinction, using σ indiscriminately.

The part of g_{f} that is due to the suppression of undulations by tension can be calculated from the relative contraction of base area, $\Delta A/A_0 < 0$, due to the undulations [13]. Here and in the following, A_0 is the real membrane area in the absence of lateral tension, while ΔA is the difference between the projected area A and A_0 . Considering a square piece of membrane, we have for a single mode the relative change

$$\left(\frac{\Delta A}{A_0} \right)_{\vec{q}} = -\frac{1}{2} q^2 \langle |u_{\vec{q}}|^2 \rangle. \quad (27)$$

Integration over the \vec{q} plane yields, because of (9),

$$\frac{\Delta A}{A_0} = -\frac{kT}{8\pi\kappa} \ln \frac{\pi^2/a^2 + \sigma/\kappa}{\pi^2/A_0 + \sigma/\kappa} \quad (28)$$

where the molecular length a controls the upper cutoff wave vector π/a . For a wide range of tensions, $\kappa\pi^2/A_0 < \sigma < \kappa\pi^2/a^2$, eq. (28) simplifies to

$$\frac{\Delta A}{A_0} = -\frac{kT}{8\pi\kappa} \ln \frac{\kappa\pi^2}{\sigma a^2} \quad (29)$$

which no longer depends on A_0 . Obviously, $\Delta A/A_0$ increases towards zero as the tension goes up. Stretching of undulations has to be complemented by Hookean stretching, $\Delta A/A_0 = \sigma/\lambda \geq 0$, where λ is the stretching modulus of the bilayer. Inserting both contributions into the differential energy balance

$$dg_f = \sigma \frac{d(\Delta A/A_0)}{d\sigma} d\sigma \quad (30)$$

we obtain

$$g_f = \frac{kT}{8\pi\kappa} \sigma + \frac{1}{2\lambda} \sigma^2. \quad (31)$$

The Hookean term can be neglected for the tensions of interest, $10^{-6} \text{ mN/m} < \sigma < 10^{-3} \text{ mN/m}$, as λ was measured to be about 200 mN/m for the lipid membranes of our studies [24]. (These tensions are also far below $\kappa\pi^2/a^2$, the upper limit of validity of (29).) We do not try to calculate the energy of the bound state, g_b . However, it is easy to realize that g_b must be positive because otherwise the membrane would adhere spontaneously. This and the omission of the Hookean term permit us to deduce from eq. (25) the inequality

$$g_{ad} < \frac{kT}{8\pi\kappa} \sigma. \quad (32)$$

For a numerical comparison of the two relationships for the adhesion energy, (5) and (32), we focus on EYPC bilayers. The bending rigidity of no other fluid membrane has been measured more often, by more experimental methods, and with the results varying more widely. The mean values of different studies are spread over a power of ten, namely $\kappa = (0.24 - 2.3) \times 10^{-19} \text{ J}$ [35–37] (see also below). Using these numbers and, in addition, the contact angle of the single PC membrane adhering to a bundle, $\psi = 70^\circ$, and the room temperature value $kT = 4 \times 10^{-21} \text{ J}$, we obtain from the Young equation (5)

$$g_{ad} = 0.66\sigma \quad (33)$$

and from the inequality (32)

$$g_{ad} < (0.66 - 6.6) \times 10^{-3}\sigma. \quad (34)$$

Evidently, there is a glaring discrepancy of two or three orders of magnitude between the two formulas. It is reduced only by a factor of three for symmetric adhesion with $\psi = 40^\circ$. Similar contradictions are found for PE and DGDG membranes.

The conflict is mitigated but not removed if the changes in membrane area are taken into account. With $\alpha = A/A_0$ denoting the ratio of projected area at arbitrary σ to real area at $\sigma = 0$, one easily finds the corrected Young equation

$$\alpha_b g_{\text{ad}} = (\alpha_f - \alpha_b \cos \psi) \sigma \quad (35)$$

and the corrected other energy balance

$$\alpha_b g_{\text{ad}} = (\alpha_f g_f - \alpha_b g_b) \quad (36)$$

for adhesion of the single membrane to the stack. The energies g refer to unit projected area, while their products with the respective α refer to unit real area at $\sigma = 0$. Let us rewrite (35) as

$$g_{\text{ad}} = \left(\frac{\alpha_f}{\alpha_b} - \cos \psi \right) \sigma \quad (37)$$

and keep of (36) the only inequality

$$g_{\text{ad}} < \frac{\alpha_f}{\alpha_b} g_f \quad (38)$$

where again use is made of $g_b > 0$. The last two relationships replace (5) and (32). Neglecting Hookean elasticity, i.e. taking the real area to be fixed, and using (29), one has

$$\alpha_f = \left(1 + \frac{\Delta A}{A_0} \right) = 1 - \frac{kT}{8\pi\kappa} \ln \frac{\kappa\pi^2}{\sigma a^2} < 1. \quad (39)$$

A new, improved calculation starting from the product of the correction factors for all the modes,

$$\frac{\Delta A}{A_0} = \prod_{\vec{q}} \left[1 - \left(\frac{\Delta A}{A_0} \right)_{\vec{q}} \right], \quad (40)$$

gives

$$\alpha_f = \frac{1}{1 + \frac{kT}{8\pi\kappa} \ln \frac{\kappa\pi^2}{\sigma a^2}} \quad (41)$$

which becomes (39) again for $\alpha_f \rightarrow 1$. With $\kappa = 0.24 \times 10^{-19}$ (the lowest experimental value), $a = 1$ nm, $\sigma = 1 \times 10^{-5}$ mN/m and room temperature, we find from (41) $\alpha_f = 0.90$ which may be regarded as a lower limit to α_f for EYPC.

Finally, we write down a differential equation for the energy of undulation stretching per unit real area of free membrane which follows from (41) and replaces (30)

$$d(\alpha_f g_f) = \sigma \frac{d\alpha_f}{d\sigma} d\sigma = \frac{\frac{kT}{8\pi\kappa}}{\left(1 + \frac{kT}{8\pi\kappa} \ln \frac{\kappa\pi^2}{\sigma a^2}\right)^2} d\sigma. \quad (42)$$

From (41) and (42) one obtains the inequality

$$\alpha_f g_f < \alpha_f^2 \frac{kT}{8\pi\kappa} \sigma \quad (43)$$

and, in combination with (38),

$$g_{ad} < \frac{\alpha_f^2}{\alpha_b} \frac{kT}{8\pi\kappa} \sigma. \quad (44)$$

For a conservative comparison of (37) and (44) we assume the most favorable case, $\alpha_b = 1$, in (37) and replace α_f^2/α_b by unity in (44). Inspection for EYPC shows that this reduces the discrepancy between the Young equation and the other energy balance only marginally for the single membrane adhering to a stack of other membranes. The situation is similar for symmetric pair adhesion of EYPC membranes and for both kinds of adhesion of PE and DGDG bilayers.

In order to bridge the gap between the Young equation and the other energy balance, we postulated an anomalous roughness of the investigated lipid membranes which stores much more membrane area than do the thermal undulations. A natural way of dealing with such an extra roughness, suggested by the agreement of experimental and theoretical scaling laws, is to use the same formulas as above but adopt a hypothetical κ much smaller than the measured values. A dramatic reduction of the hypothetical bending rigidity down to about 3×10^{-21} J, for EYPC would be required to make inequality (44) compatible with (38). This would imply $\alpha_f \approx 0.4$ or, in other words, a stored area 1.5 times the base area. Less storage but an even smaller hypothetical κ may be inferred from the argument that the superstructure could have a larger cutoff length in (41) than the molecular length a . In any event, the stored area has to be several times the 10% of the base area ($\alpha_f = 0.90$) which we maximally estimated for the undulations of EYPC bilayers.

From the experiments with EYPC multilayer systems we obtained $\langle z \rangle_{eq} = 10$ nm at a tension which initially was estimated at 10^{-4} mN/m. With $\kappa = 2.4 \times 10^{-20}$ J, instead of the 1×10^{-19} J used originally, the tension decreases proportionally. Insertion of these tensions, besides $\langle z \rangle_{eq}$, into (20) leads to Hamaker constants less than 4 or 1% below its critical value. This is another result that is difficult to reconcile with undulation theory as it means that very small parameter changes would have been sufficient to cause spontaneous adhesion which we never saw. (A further argument to this effect [6], assuming a collapse rather than a gradual decrease of the net repulsion with increasing H , is incorrect.) We may conclude from the estimate that the anomalous roughness is much more sensitive to lateral tension than would be standard undulations producing the same equilibrium mean spacing.

5. Other indications of lipid membrane complexity and superstructure

In our light microscopic studies of induced adhesion we did not see any superstructure or anomalous roughness and, for a long time, suspected none. However, there are some observations pointing to complexities of lipid membranes which are older than the contradictions of induced adhesion. The first serious indication of anomalous mechanical properties of PC membranes emerged in measurements of the bending rigidity [36]. Registering the fluctuations of the angle made by the ends of tubular PC vesicles, we noticed in addition intermittent rapid wiggle-like fluctuations of the tubes which were stronger with distearoyl PC (DSPC) than with shorter-chain saturated PC's and EYPC. The wiggles disappeared within a second and after a few seconds reappeared usually in another section of the tube; they rarely covered the whole length of it. Sometimes we also saw a knee which lasted up to 4 s and could migrate along the tube. Estimating the bending energies of wiggles and knees on the basis of the bending rigidity derived from the mean square fluctuation angle, $\kappa \approx 2 \times 10^{-19}$ J, we found these energies much too high for thermal excitation. The lower bending rigidities measured in the meantime with other methods may reduce the energies to acceptable levels, but the intermittency of the wiggles can still not be explained in terms of undulations and their relaxation.

Another strange property of EYPC bilayers is the existence of a dispersive phase [23]. It forms in the highly swollen multilayer systems displaying induced adhesion upon cooling. When these samples are annealed for several hours at less than 15 °C, the planar multilayer system breaks up into water chambers separated by one or more membranes. Subsequently raising the temperature beyond 15 °C results in the precipitation of many flakes in each chamber which display Brownian motion and rapidly fuse to form one 'dark body' per chamber. These spherelike bodies are probably made of a single multiply self-connected membrane. When the temperature is decreased below 15 °C again, the dark bodies fade and the dispersive phase is reestablished. The nature of the dispersive phase is still unknown, but its existence and its reversible transformation are evidence for an amazing complexity of EYPC membranes. A dispersion contrasts sharply with the fact that, when stressed, the EYPC membranes rupture only at tensions of (3–4) mN/m [23].

There is a third phenomenon, well-known and discovered early on by Evans [38], which possibly hints at anomalous membrane properties. Micromanipulation reveals that vesicles tend to be connected by microscopically invisible tethers. Their presence becomes apparent only when a vesicle is aspirated by the micropipette and pulled away. Tethers are thought to be thin tubes formed by the highly curved membrane. If the energy of tube formation equals the regular bending energy of a cylinder, the tube has to be stabilized (in the absence of spontaneous curvature) by a pull of the force $2\pi\kappa/r$, r being the radius [39]. Since it is difficult to understand the origin of these forces one may wonder whether the tethers are possibly stabilized by some unknown property of the membrane. Another reason to suspect such a stabilization is the occurrence of huge batteries of tubes, at first too thin to be optically resolved, in dilute EYPC samples during the swelling process [40].

The contradictions that arose in the quantitative analysis of induced adhesion carry more weight than those precursory observations. They were obtained with the bilayers of many different lipids and they are based on experiments which are in part controllable and yield physical quantities such as contact angles, lateral tensions and mean spacings. We see no possibility of removing the conflict other than to postulate an anomalous roughness of the membranes which, in turn, has to be supported by a membrane superstructure. The most direct method to search for these two membrane features is cryo-transmission electron microscopy. Fortunately, E. Zeitler permitted us to do such studies at the Fritz-Haber-Institut. In early 1988 we obtained the first electron micrograph showing EYPC vesicles with grainy membranes. The typical 'period' of the irregular black and white pattern is about 5 nm. Encouraged by the pictures, we proposed also in 1988 a tentative model for the superstructure [41]. Its basic element is a local saddle deformation about as large as the membrane thickness of ca. 4 nm. The saddle is stabilized by higher order bending elasticity so that an energy barrier has to be overcome to create or destroy it. Each saddle in an otherwise flat membrane is surrounded by two highs and two lows which the saddles should tend to share in order to save regular bending energy. The resulting cooperativity of the saddles may be expected to give rise to membrane deformations on a scale larger than a saddle, thus creating most of the anomalous roughness. Lateral tension above a certain threshold should lead to the destruction of the superstructure, leaving a rather smooth membrane which still performs thermal undulations. When the tension is turned off, the superstructure will reappear in the course of time. In such a model, the anomalous roughness depends on the history of the membrane and is sensitive to lateral tension and, perhaps, other factors.

The first electron micrograph showing an EYPC vesicle with a grainy membrane was presented at a conference in 1989 [42]. While the vesicles displaying grainy membranes were nearly spherical, we obtained in early 1990 angular EYPC vesicles [43, 44]. Their shapes differ markedly from those seen in light microscopy despite the theoretical scale invariance of vesicle shapes. We think that the angularity is an example of the anomalous roughness for which we were looking. The lack of graininess in these membranes, and the general rarity of grainy membranes, is attributed to the leveling action of the high lateral tensions that arise during the rapid freezing of the samples. The tensions, a consequence of the large thermal expansivity of lipid membranes [24], are manifested by a number of artefacts. A comprehensive description of the results obtained so far with cryo-transmission electron microscopy has just been published [45].

Other authors made some similar observations with cryo-transmission electron microscopy. The graininess has recently been found by Lücken and Jäger in vesicular membranes of EYPC, soya PC, and DMPC, each containing some cholesterol [46]. Small (100 nm long) elongated vesicles with a sharp notch on one side, resembling hearts apart from the missing tip, have been seen in the Sackmann group in samples of pure DMPC [47], while we found an EYPC vesicle with such a shape [45]. The notches appear to be very pronounced, highly localized saddles.

In another attempt to prove the existence of an anomalous roughness in a direct manner we measured the apparent membrane area as a function of lateral tension

by deforming fluctuating spherical vesicles into prolate ellipsoids with electric fields (which simultaneously lifted them from the object slide) [37]. This is a very gentle method as there is no lower limit to the lateral tension produced by the Maxwell stresses and its upper limit is about 10^{-3} mN/m. Plotting area versus the logarithm of tension usually resulted in straight lines as predicted by (29). The bending rigidities computed from the slopes were the lowest ever recorded for the six lipids studied, ranging from 3.4×10^{-20} J for dilauroyl PC to 1.1×10^{-20} J for DGDG, with EYPC and three other PC's including stearylloleoyl PC (SOPC) in between [37]. Interestingly, some of the palmitoylloleoyl PC and EYPC vesicles could be stretched, reversible and without hysteresis, by up to 17% instead of the typical 2 to 5%. The large increase in area suggests the presence of a substantial anomalous roughness. Plotting these areas as usual versus the logarithm of tension resulted in S-shaped curves, but plotting them versus the logarithm of the squared field strength gave straight lines again (except at the lowest fields) the slopes of which suggest a bending rigidity of ca. $(1/3)kT$. The very low value is of the order of our estimate of the effective bending rigidity which would be needed to remove one of the contradictions of induced adhesion.

The difficulties of measuring the bending rigidities of lipid bilayers may also point to complex behavior. The mean values of κ obtained in different studies seem to depend on the experimental method. The largest values were derived from the bending fluctuations (uniform bending mode) of tubular vesicles [35, 36] while the smallest were computed from the electric deformation of spherical vesicles [37]. Intermediate values resulted from the fluctuation mode analysis of spherical vesicles [48]. The largest and smallest mean values were seen to differ by a factor of ten in the case of EYPC, the only lipid bilayer whose bending rigidity was measured with both fluctuating tubes and electrically deformed spheres. It is not only the disagreement between the mean values found by different methods that poses a problem. In addition, it appears to be typical of most methods that in a series of equal experiments the scatter of κ as measured with different vesicles is larger than the error of κ as obtained from a single vesicle.

If there is a bilayer superstructure, it could provide an explanation for the uncertainties of the bending rigidity. A dependence of the superstructure on membrane geometry could manifest itself in a disagreement of the results obtained with different methods and a dependence on the vesicle's history would produce scatter. Moreover, the superstructure could make the bending rigidity depend on fluctuation wavelength. Obviously, a disordered superstructure offers a bewildering multitude of theoretical possibilities. Specific assignments seem premature as long as we know almost nothing about the effects of impurities and temperature on the bending rigidity. The membrane may be contaminated by glues, perhaps even silicone greases, and by chemical degradation. Angelova et al. reported a decrease of the bending rigidity of EYPC from 0.7 to 0.5×10^{-19} J in the course of two weeks [49]. In recent comparative measurements we found a systematic difference between the bending rigidities obtained with two different methods from the same spherical vesicles [50]. We also noted in these studies that the very low values of κ extracted from the

electric deformation of spheres rose by a factor of two when the glue was separated from the sample by a barrier of silicone grease.

A dramatic change of the intrinsic bending rigidity by impurities dissolved in the bilayer seems unlikely. However, impurities inducing a local spontaneous bilayer curvature can reduce its bending rigidity to very low values [51, 52]. In a microscopic picture, each such impurity molecule produces a mobile hat in the membrane [41, 53]. In contrast, the superstructure is thought to be built from local saddles. One of the reasons for this assumption is that the superstructure does not appear to have a dramatic effect on the bending rigidity. Both a decrease and an increase of the bending rigidity are conceivable consequences, depending on whether the superstructure mainly rigidifies or roughens the bilayer. A superstructure may also be very sensitive to impurities.

Rather well reproducible values of κ seem to have been measured when the vesicles were aspirated with a micropipette. In one of two such studies, κ was computed, by use of (29), from the apparent membrane stretching as a function of lateral tension [54]. In another experiment, a tether was pulled from a vesicle held by a micropipette and κ was calculated from the tether radius and the pulling force [39]. The results of the two methods can be compared for stearyloleoyl phosphatidylcholine (SOPC), a lipid similar to EYPC, κ being $(0.90 \pm 0.06) \times 10^{-19}$ J and $(1.20 \pm 0.17) \times 10^{-19}$ J, respectively. One may speculate that the small errors and the good agreement of these results are due to the high lateral tensions occurring in these experiments. They could easily be sufficient to destroy anomalous roughness and superstructure, which leaves membranes that are roughened only by the thermal undulations controlled by bending rigidity and lateral tension. The electric deformation [37] and the fluctuation mode analysis [55] of spherical vesicles yielded 0.26×10^{-19} J $\pm 20\%$ and 1.4×10^{-19} J $\pm 20\%$, respectively.

High lateral tension produced by vesicle aspiration (and perhaps by other steps in the preparation of samples for micromanipulation) may also explain why Evans appears to find spontaneous adhesion while we do not, the conflict noted in the Introduction. We suspect that Evans' membranes lost the superstructure before or during the measurements, while ours kept it as they were not manipulated. The smoother the membranes, the more likely they are to spontaneously adhere to each other. Therefore, it is tempting to conclude that the postulated superstructure, regardless of how much anomalous roughness it generates, is a precondition for membrane separation. Such an interpretation is supported by the finding that the X-ray signal indicating the period of a multilayer system does not shift or broaden after the initial absorption of water, but vanishes gradually in those cases where the swelling continues [56]. We suspect that the multilayer system stops water uptake upon reaching the so-called equilibrium spacing, with the outermost membranes tending to peel off when the absence of constraints permits them to assume the superstructure.

According to this model the adhesion observed by Evans is, in a strict sense, not spontaneous but induced by high lateral tension applied previously (or simultaneously). Therefore, the energy of adhesion should be lower than the energy of stretching the adhering pieces of membrane prior to their mutual adhesion. A substantial fraction of the stretching energy would be used in this case to level

the superstructure, because the real (Hookean) stretching of the tight membrane at $\sigma = 1$ mN/m does not bind enough energy. In other words, it seems impossible to explain the adhesion energies measured by Evans in terms of asymmetric induced adhesion without invoking the superstructure.

Finally, circumstantial evidence for membrane complexity is possibly provided by vesicle budding. The formation of a mother-daughter pair, i.e. two spheres of different size connected by a narrow constriction, usually starts from an ellipsoidal shape. In the experiments of Käs et al. budding was driven by a rising temperature and typically proceeded through asymmetric shapes such as eggs and pears [57, 58]. A continuous transition through these shapes is predicted by the so-called bilayer-couple model [57, 59, 60]. According to the model, a shape independent difference in area between the monolayers forming the bilayer is the control parameter of the transition and determines the equilibrium shapes at a given stage. An alternative model, in which a shape independent spontaneous curvature of the bilayer assumes the role of the control parameter, predicts an abrupt transition from the ellipsoid to the mother-daughter pair [59–61]. There is also a complete model that takes monolayer stretching and its energy into account and comprises the two other models as limiting cases [62–64]. Starting from the complete model and the bilayer stretching moduli as measured by Evans [3, 24, 54], we showed that budding should closely follow the spontaneous curvature model, in contrast with the prevailing experimental process [65]. Käs and Sackmann took care that they had equilibrium shapes by increasing the temperature only very slowly, sometimes in steps of 0.1 K at intervals of 15 minutes [58]. Barring the possibility that the eggs and pears were fluctuations taking the vesicle up to and over an energy barrier [66], their observation appears to be another sign of complex mechanical properties which are not part of our usual picture of these membranes. The impression of complexity is reinforced by other irregularities of budding reported by Käs et al. [58] and by us [65]. Moreover, E. Evans found that upon increasing the membrane area by raising the temperature vesicles can erupt to form fully connected highly irregular structures, among them outward and inward buds on the same membrane [38, 54].

6. Conclusion

The present article has been written with great hesitation. On the one hand, it seems useful to discuss the puzzles of vesicular lipid membranes. This may speed up their resolution by new experiments and theories. On the other hand, the concepts put forward to solve the problems raise many questions which should be addressed first in order to avoid serious mistakes. We have not yet seen grainy membranes and angular vesicles of a one-component lipid, and we would like to know the time taken by the unstressed single membrane to develop the conjectured superstructure. Clearly, it is much too early for an authoritative review. To convince (or persuade) the reader of superstructure and anomalous roughness, adhesion induced by lateral tension, on which there is a large body of data, has been elaborated with estimates. However, the result of these estimates, a stored excess area about as large as the

projected area or larger, is disquieting in view of the scanty evidence provided by angular vesicles and very stretchable membranes. The last part of this article is a list of intriguing observations which seem to suggest a membrane superstructure or, at least, membrane complexity.

It is an interesting question if nature makes use of induced adhesion in cell biology. The large and tension independent contact angles of induced adhesion would permit extended and rather stable contact of plasma membranes. Induced adhesion has the advantage over spontaneous adhesion that it is terminated when the tension becomes zero. From a general point of view, complex behavior could enable lipid membranes to perform many different and even seemingly contradictory functions. Were the lipids which we investigated, i.e. PC, PE and DGDG, selected by nature for engineering purposes? If so, are their special properties still needed in the presence of highly evolved proteins which control most membrane functions? We do not know the answers, but think that the bilayers of typical biological lipids, being the matrix for these proteins, deserve very careful examination.

Acknowledgements

My thanks go to my students and coworkers who were willing to do so many explorations into the field of lipid membranes. It was their discoveries which allowed me to play with theoretical models for these mysterious systems. I am particularly grateful to W. Harbich and R.M. Servuss who were the pioneers and spent very many years in my group. More recently, M. Mutz and M. Kummrow continued the explorative work. The search for superstructure and anomalous roughness by cryo-transmission electron microscopy is being carried out by B. Klösgen who joined the group as a postdoc. The work was supported in a large measure by the Deutsche Forschungsgemeinschaft through personal research grants and Sonderforschungsbereich 312.

References

1. LeNeveu, D.M., R.P. Rand, V.A. Parsegian and R.P. Gingell, 1977, Measurement and modification of forces between lecithin bilayers, *Biophys. J.* **18**, 209–230.
2. Evans, E. and M. Metcalfe, 1984, Free energy potential for aggregation of giant, neutral lipid bilayer vesicles by van der Waals attraction, *Biophys. J.* **46**, 423–426.
3. Evans, E. and D. Needham, 1987, Physical properties of surfactant bilayer membranes: Thermal transitions, elasticity, rigidity, cohesion, and colloidal interactions, *J. Phys. Chem.* **91**, 4219–4228.
4. Lipowsky, R. and S. Leibler, 1986, Unbinding transitions of interacting membranes, *Phys. Rev. Lett.* **56**, 2541–2544.
5. Lipowsky, R. and S. Leibler, 1987, Erratum, *Phys. Rev. Lett.* **59**, 1983.
6. For a review, see R. Lipowsky, *Statistical physics of flexible membranes*, 1993, *Physica A* **194**, 114–127.
7. Helfrich, W., 1989, Spontaneous and induced adhesion of fluid membranes, in: *Phase Transitions of Soft Matter*, eds T. Riste and D. Sherrington (Plenum, New York) pp. 271–281.
8. Milner, S.T. and D. Roux, 1992, Flory theory of the unbinding transition, *J. Phys. I France* **2**, 1741–1754.
9. Helfrich, W., 1993, Mean-field theory of n-layer unbinding, *J. Phys. II France* **3**, 385–393.
10. Burkhardt, T.W. and P. Schlottmann, 1993, Unbinding transition in a many-string system, *J. Phys. A* **26**, L 501.
11. Lipowsky, R., 1988, Lines of renormalization group fixed points for fluid crystalline membranes, *Europhys. Lett.* **7**, 255–261.

11. Cook-Röder, J. and R. Lipowsky, 1992, Adhesion and unbinding of bunches of fluid membranes, *Europhys. Lett.* **18**, 433–438.
Netz, R.R. and R. Lipowsky, Critical behavior of three interacting strings, 1993, *Phys. Rev. E* **47**, 3039.
Netz, R.R. and R. Lipowsky, Three interacting strings in two dimensions: Nonuniversal and multiple unbinding transitions, *J. Phys. I (France)*, submitted.
Netz, R.R. and R. Lipowsky, 1993, The unbinding of symmetric and asymmetric stacks of membranes, *Phys. Rev. Lett.* **21**, 3596–3599.
12. Mutz, M. and W. Helfrich, 1989, Unbinding transition of a biological model membrane, *Phys. Rev. Lett.* **62**, 2881–2884.
13. Helfrich, W. and R.M. Servuss, 1984, Undulations, steric interaction and cohesion of fluid membranes, *Il Nuovo Cimento D* **3**, 137–151.
14. Servuss, R.M. and W. Helfrich, 1987, Undulation forces and the cohesion energy of egg lecithin membranes, in: *Physics of Complex and Supermolecular Fluids*, eds S.A. Safran and N.A. Clark, (Wiley, New York) pp. 85–100.
15. Servuss, R.M. and W. Helfrich, 1989, Mutual adhesion of lecithin membranes at ultralow tensions, *J. Phys. France* **50**, 809–827.
16. Harbich, W. and W. Helfrich, 1990, Adhesion of egg lecithin multilayer systems produced by cooling, *J. Phys. France* **51**, 1027–1048.
17. Mutz, M., R.M. Servuss and W. Helfrich, 1990, Giant membranes of swollen phosphatidylethanolamines and glycolipids, *J. Phys. France* **51**, 2557–2570.
18. Lipowsky, R. and U. Seifert, 1991, Adhesion of membranes: A theoretical perspective, *Langmuir* **7**, 1867–1873.
19. Helfrich, W. and W. Harbich, 1985, Adhesion and cohesion of tubular vesicles, *Chem. Scr.* **25**, 32–36.
20. Bailey, S.M., S. Chiruvolu, J.N. Israelachvili and J.A. Zasadzinski, 1990, Measurements of forces involved in vesicle adhesion using freeze-fracture electron microscopy, *Langmuir* **6**, 1326–1329.
21. Helm, C., J.N. Israelachvili, P.M. McGuiggan, 1992, Role of hydrophobic forces in bilayer adhesion and fusion, *Biochemistry* **31**, 1794–1805.
22. Harbich, W. and W. Helfrich, 1984, The swelling of egg lecithin in water, *Chem. Phys. Lipids* **36**, 39–63.
23. Harbich, W. and W. Helfrich, 1990, Phases of egg phosphatidylcholine in an abundance of water, *Chem. Phys. Lipids* **55**, 191–205.
24. Kwok, R. and E. Evans, 1981, Thermoelasticity of large lecithin bilayer vesicles, *Biophys. J.* **35**, 637–652.
25. See, e.g., Mahanta J. and B.W. Ninham, 1976, *Dispersion Forces* (Academic Press).
26. See, e.g., Rand R.P. and A. Parsegian, 1989, Hydration forces between phospholipid bilayers, *Biochim. Biophys. Acta* **988**, 351–376.
27. Helfrich, W., 1978, Steric interaction of fluid membranes in multilayer systems, *Z. Naturforsch.* **33a**, 305–315.
28. Safinya, C.R., D. Roux, G.S. Smith, S.K. Sinha, P. Dimon, N.A. Clark and A.M. Bellocq, 1986, Steric interaction in a model multimembrane system: A synchrotron X-ray study, *Phys. Rev. Lett.* **57**, 2518–2521.
29. Bassereau, P., J. Marnigand and G. Porte, 1987, An X-ray study of brine swollen lyotropic lamellar phases, *J. Physique* **48**, 673–678.
Porte, J., 1992, Lamellar phases and disordered phases of fluid bilayer membranes, *J. Phys.: Cond. Matter* **4**, 8649–8670 (review).
30. Janke, W., 1990, Entropic repulsion between fluctuating surfaces, *Int. J. Modern Phys.* **B4**, 1763–1808 (review).
31. Kleinert, H. and W. Janke, 1987, Fluctuation pressure of a stack of membranes, *Phys. Rev. Lett.* **58**, 144–147.
32. Gompper, G. and D.M. Kroll, 1989, Steric interactions in multilamellar systems: A Monte Carlo study, *Europhys. Lett.* **9**, 59–64.

33. David, F., 1990, Renormalization group treatment of entropic interactions in lamellar phases, Colloque de Physique **C7**, 115–129 (supplement to J. Phys. France **51**).
34. Sornette, D., 1986, Steric Interaction between wandering walls: study of the strong deviation from mean-field theory, Europhys. Lett. **2**, 715–724.
35. Servuss, R.M., W. Harbich and W. Helfrich, 1976, Measurement of the curvature-elastic modulus of egg lecithin bilayers, Biochim. Biophys. Acta **436**, 900–903.
36. Beblík, G., R.M. Servuss and W. Helfrich, 1985, Bilayer bending rigidity of some synthetic lecithins, J. Physique **46**, 1773–1778.
37. Kummrow, M. and W. Helfrich, 1991, Deformation of giant lipid vesicles by electric fields, Phys. Rev. A. **44**, 8356–8360.
Kummrow, M., 1992, Lichtmikroskopische Untersuchungen zur Deformation biologischer Modellmembranen im elektrischen Feld. Dissertation, Fachbereich Physik, Freie Universität Berlin.
38. E. Evans, Private communication.
39. Waugh, R.E., J. Song, S. Svetina and B. Žekš, 1992, Local and nonlocal curvature elasticity in bilayer membranes by tether formation from lecithin vesicles, Biophys. J. **61**, 974–982.
40. Servuss, R.M., 1989, Local and nonlocal curvature elasticity in bilayer membranes by tether formation from lecithin vesicles, Color scatterers in egg lecithin water systems, Chem. Phys. Lipids **50**, 87–97.
41. Helfrich, W., 1989, Hats and saddles in lipid membranes, Liq. Cryst. **5**, 1647–1658.
42. Helfrich, W. and B. Klösgen, 1990, Adhesion and roughness of biological model membranes, in: Dynamics and Patterns in Complex Fluids, eds A. Onuki and K. Kawasaki, Springer Proc. Phys. **52**, 2–18.
43. Helfrich, W. and B. Klösgen, 1993, Some complexities of simple lipid membranes, in: Proceedings of the Workshop on Dynamical Phenomena at Surfaces, Interfaces and Membranes, Les Houches 1991, eds D. Beysens, N. Boccaro and G. Forgacs (Nova Science Publishers, Commack, NY) pp. 211–220.
44. Klösgen, B. and W. Helfrich, 1992, Electron microscopy of biological model membranes, in: The Structure and Conformation of Amphiphilic Membranes, eds R. Lipowsky, D. Richter and K. Kremer, Springer Proc. Phys. **66**, 105–112.
45. Klösgen, B. and W. Helfrich, 1993, Special features of phosphatidylcholine vesicles as seen in cryo-transmission electron microscopy, Eur. Biophys. J. **22**, 329–340.
46. Lücken, U. and J. Jäger, 1992, The structure of membranes and membrane proteins embedded in amorphous ice, in: Proc. 50th Annual Meeting of the Electron Microscopy Society of America, eds G.W. Bailey, J. Bentley and J.A. Small (San Francisco Press, San Francisco) pp. 432–433, and private communication.
47. Weiss, A., 1989, Kryo-Elektronenmikroskopie an Phospholipidvesikeln. Diplomarbeit, Fakultät für Physik, Technische Universität München.
48. Faucon, J.F., M.D. Mitov, P. Méléard, I. Bivas and P. Bothorel, 1989, Bending elasticity and thermal fluctuations of lipid membranes: Theoretical and experimental requirements, J. Phys. France **50**, 2389–2397.
49. Angelova, M.I., S. Soléau, Ph. Méléard, J.F. Faucon and P. Bothorel, 1992, Preparation of giant vesicles by external AC fields: Kinetics and application, Colloid Polym. Sci. **89**, 127.
50. Niggemann, G., M. Kummrow and W. Helfrich, to be published.
51. Safran, S.A., P. Pincus and D. Andelman, 1990, Theory of spontaneous vesicle formation in surfactant mixtures, Science **248**, 345–356.
52. Kozlov, M.M. and W. Helfrich, 1992, Effects of a cosurfactant on the stretching and bending elasticities of a surfactant monolayer, Langmuir **8**, 2792–2797.
53. Helfrich, W. and M.M. Kozlov, 1994, Flexibility and roughness of mixed and partially polymerized bilayers in terms of the hat model and local bending frustration, J. Phys. France II. **4**, 1427.
54. Evans, E. and B. Rawicz, 1990, Entropy-driven tension and bending elasticity in condensed-fluid membranes, Phys. Rev. Lett. **64**, 2094–2097.
55. Häckl, W., 1994, Anwendung der computergestützten Mikroskopie zur Messung von elastischen Eigenschaften von Membranen. Diplomarbeit, Fakultät für Physik, Technische Universität München. **49**, 77.

56. Hartung, J., W. Helfrich and B. Klösgen, 1994, Transformation of phosphatidylcholine multilayer systems in excess water, *Biophys. Chem.* **49**, 77.
57. Berndt, K., J. Käs, R. Lipowsky, E. Sackmann and U. Seifert, 1990, Shape transformations of giant vesicles: extreme sensitivity to bilayer asymmetry, *Europhys. Lett.* **13**, 659–664.
58. Käs, J. and E. Sackmann, 1991, Shape transitions and shape stability of giant phospholipid vesicles in pure water induced by area-to-volume changes, *Biophys. J.* **60**, 825–844.
59. Seifert, U., K. Berndt and R. Lipowsky, 1991, Shape transformations of vesicles: phase diagram for spontaneous-curvature and bilayer-coupling model, *Phys. Rev. A* **44**, 1182–1202.
60. Miao, L., B. Fourcade, M. Rao, M. Wortis and R.K.P. Zia, 1991, Equilibrium budding and vesiculation in the curvature model of fluid membranes, *Phys. Rev. A* **43**, 6843–6856.
61. Wiese, W. and W. Helfrich, 1990, Theory of vesicle budding, *J. Phys.: Cond. Matter* **2**, SA329–SA332.
62. Helfrich, W., 1974, Blocked lipid exchange in bilayers and its possible influence on the shape of vesicles, *Z. Naturforsch.* **29c**, 510–515.
63. Evans, E., 1974, Bending resistance and chemically induced moments in membrane bilayers, *Biophys. J.* **14**, 923–931.
64. Svetina, S., M. Brumen and B. Žekš, 1985, Lipid bilayer elasticity and the bilayer couple interpretation of red cell shape transformations and lysis, *Stud. Biophys.* **110**, 177–184.
65. Wiese, W., W. Harbich and W. Helfrich, 1992, Budding of lipid bilayer vesicles and flat membranes, *J. Phys.: Condens. Matter* **4**, 1647–1657.
66. Miao, L., U. Seifert, M. Wortis and H.G. Döbereiner, 1994, Budding transitions of fluid bilayer vesicles: the effect of area difference elasticity, *Phys. Rev. E* **49**, 5389.